ELSEVIER

International Journal of Mass Spectrometry 223–224 (2003) 327–334

International Journal of Mass Spectrometry

www.elsevier.com/locate/ijms

The charge-excitation exchange process: $He^+(^2S) + Ar^*(^3P) \rightarrow He^*(^{3,1}S) + Ar^+(^2P)$

Davide Bassi [a], Stefano Falcinelli [b,c], Fernando Pirani [c,d], Barbara Rapaccini [e], Paolo Tosi [a,*], Franco Vecchiocattivi [b], Marco Vecchiocattivi [a]

[a] *Dipartimento di Fisica and Unità INFM, Università di Trento, I-38050 Povo, Italy*
[b] *Dipartimento d'Ingegneria Civile ed Ambientale, Università di Perugia, I-06125 Perugia, Italy*
[c] *Unità INFM, Università di Perugia, I-06123 Perugia, Italy*
[d] *Dipartimento di Chimica, Università di Perugia, I-06123 Perugia, Italy*
[e] *Department of Molecular and Laser Physics, University of Nijmegen, NL-6500 GL Nijmegen, The Netherlands*

Received 11 March 2002; accepted 16 May 2002

Abstract

The electron and excitation exchange reaction $Ar^*(^3P) + He^+(^2S) \rightarrow Ar^+(^2P) + He^*(2^{1,3}S)$ has been observed in a preliminary crossed beam experiment, at a collision energy of ∼10 eV. The dynamics of this process has been investigated theoretically by evaluating the diabatic potential energy curves and the relevant couplings. Transition probabilities have been calculated through the Landau–Zener–Stückelberg formula, and state-to-state cross-sections have been finally obtained. Some clues on the nature of the interaction between the reacting partners have been drawn and generalized to similar systems. (Int J Mass Spectrom 223–224 (2003) 327–334)

Keywords: Charge-excitation exchange; Charge transfer; Metastable atoms

1. Introduction

Ions and excited atoms play an important role in various kind of plasmas, which are interesting either from a physical–chemical point of view and for many technological applications. Experimental evidences have shown that most plasmas are very rich in ions, with single or double charge, and in species excited in metastable states [1]. Knowledge of the dynamics of elementary processes involving photons, electrons, ions, neutrals, and excited particles, is necessary to achieve a description of plasmas at microscopic level and to optimize methodologies for their production and utilization [2–4].

Processes involving excited atoms and ions are of great interest also in atmospheric phenomena and astrophysics. It has been observed that $He^*(2^3S)$ metastable atoms are present in large quantity in the exosphere of the earth [5,6]. Helium and neon are the predominant gaseous species in the atmosphere of red giant stars. These rare gas atoms, excited into their metastable states, are characterized by an high energy content and long lifetimes, ranging, respectively from 16.62 to 20.62 eV and from 0.02 to 4.2×10^3 s [7]. When colliding with neutral or ionic species, they can release energy by forming ions and the respective

* Corresponding author. E-mail: tosi@science.unitn.it

1387-3806/02/$ – see front matter
PII S1387-3806(02)00868-0

neutral species in the ground state [7–9]. While collisional processes of metastable atoms with atomic or molecular neutral species have been extensively investigated, much less is known on collisions between excited atoms A^* and ions B^+. In the latter case, the following reactions can occur:

$$A^* + B^+ \rightarrow A^+ + B^*$$
(electron and excitation exchange)

$$A^* + B^+ \rightarrow A^+ + B$$
(electron transfer with de-excitation)

$$A^* + B^+ \rightarrow AB^{2+} + e^- \quad \text{(associative ionization)}$$

$$A^* + B^+ \rightarrow A + B^{2+} + e^- \quad \text{(Penning ionization)}$$

$$A^* + B^+ \rightarrow A^+ + B^+ + e^-$$
(ionization with coulombic explosion)

The lack of information on the dynamics of such reactions can be probably ascribed to the difficulties of producing and manipulating simultaneously ions and metastable atoms.

In this work, we investigate the simultaneous electron and excitation exchange reaction between argon metastable atoms, $Ar^*(^3P_2, ^3P_0)$, and He^+ ions in the ground state:

$$Ar^*(^3P_2, ^3P_0) + He^+(^2S_{1/2}) \rightarrow Ar^+(^2P_{3/2}, ^2P_{1/2}) + He^*(2^1S_0, 2^3S_1) \quad (1)$$

Preliminary indications on the occurrence of reaction (1) have been obtained by using a crossed-beam apparatus [10], which produces, focuses and crosses two beams of Ar^* and He^+, in a single collision experiment. Mass spectrometry measurements with and without the He^+ ion beam have shown a difference in the Ar^+ signal, which cannot be attributed to the charge exchange between He^+ ions and ground state Ar atoms. Two different types of elementary processes are still possible: they involve the simple electron exchange or the simultaneous electron-excitation exchange. However, the asymptotic states He^+–Ar^* and He–Ar^+ are separated by about 20 eV (Fig. 1) and this makes negligible the non-adiabatic coupling between them. Consequently, the probability of a simple electron transfer vanishes. In contrast, states involved in the electron-excitation exchange are energetically close, and therefore, the probability of related reactions can be high. We can conclude that our observation of Ar^+ ion production in collisions between He^+

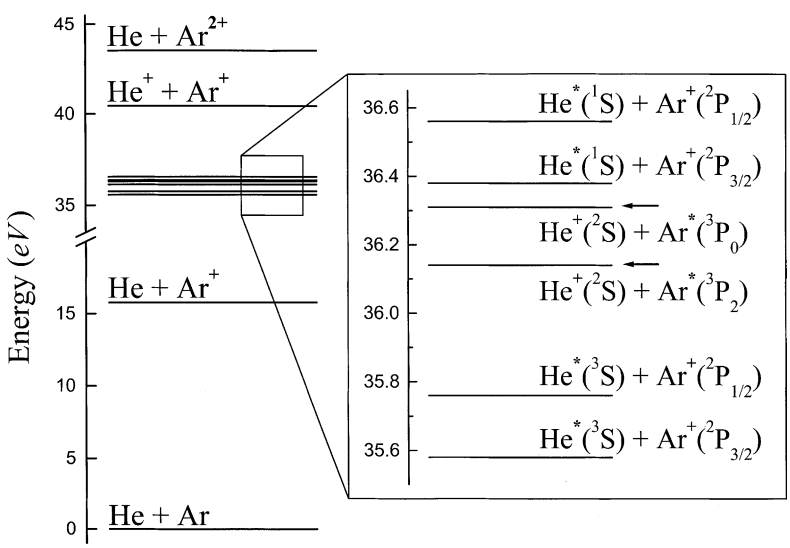

Fig. 1. Asymptotic energy levels of the relevant states. The two entrance channels are indicated by arrows.

ions and Ar* metastable atoms at an energy of ∼10 eV is referred only to reaction (1). Unfortunately, our results are still very preliminary. In particular, there is a large uncertainty concerning the effective density of the scattering target, and this limits the accuracy of the measurement. We estimate the cross-section to be about 1 Å^2, but further experimental developments are necessary to achieve a quantitative understanding of the observed processes. In addition, the authors are not aware of previous experimental studies on such system. For such reasons, we have investigated the process theoretically, with the aim to give an estimate of the cross-section and thus, to understand the feasibility of a complete experiment.

2. Theoretical description

Collision dynamics has been investigated following three steps. In the first one, the diabatic potential energy curves have been evaluated, both in the entrance and exit channels. These curves describe the interaction starting from the asymptotic atomic levels of He^+–Ar* and He*–Ar^+, but excluding electron exchange effects that arise at short and intermediate interatomic distance R. The second step concerns with the estimate of the coupling terms between potential curves; such terms depend on the charge exchange. The usefulness of such an approach for estimating the interaction consists in the intuitive physical picture of the interaction, and in the possibility of direct reference to atomic properties, like polarizability, ionization potential, electron affinity, and charge. In the final step, calculations of integral cross-sections have been performed following the Landau–Zener–Stückelberg treatment. Transition probabilities are calculated for each impact parameter, and then contributions from different impact parameters are added.

2.1. Diabatic potential energy curves

The interaction in the diabatic representation, i.e., with the excited outer electron confined on the metastable atom, has been assumed to arise from the following contributions: (i) an induction term, which represents the charge-induced multipole attraction; (ii) a dispersion term, which accounts for the induced multipole-induced multipole attraction; (iii) a repulsive term, which derives from the overlap of outer shell orbitals of the two interacting partners. The first two terms are dominant at large distances, while the third one prevails at short range. The induction term is expected to be rather large when compared to the dispersion term because of the low polarizability of the atomic ions [11] He^+ and Ar^+, with respect to the neutral metastable atoms [12] (Table 1). The characteristic parameters of the resulting potential, namely the depth of the potential well ε, and its location R_m are reported in Table 2. They have been evaluated by the use of correlation formulas, given in terms of charge and polarizability of the two separated partners [11,15,16]. In particular, the polarizability has been found to be the critical quantity for scaling both repulsion and attraction, being related to the atomic volume and to the probability of induced multipole formation. An additional repulsive term can arise at short distance due to the large difference between the

Table 1
Atomic polarizabilities and radii of ion and metastable helium and argon

	α (Å^3)	Atomic radius (Å)
$He^+(^2S_{1/2})$	0.03[a]	0.26[b]
$He^*(2^3S_1)$	47[c]	3.0[d]
$He^*(2^1S_1)$	119[c]	4.1[d]
$Ar^+(^2P_{3/2,1/2})$	0.68[a]	0.74[d]
$Ar^*(^3P_{2,0})$	48[c]	3.0[d]

[a] From [11].
[b] Calculated exactly from the Bohr formula.
[c] From [12].
[d] Calculated by exploiting the proportionality between the radius and the cubic square of polarizability [13,14].

Table 2
Lennard–Jones [4,8] potential parameters for diabatic interactions as obtained from the correlation formulas (see text)

	ε (eV)	R_m (Å)
$He^+(^2S_{1/2})$–$Ar^*(^3P_{2,0})$	0.94	4.04
$He^*(2^3S_1)$–$Ar^+(^2P_{3/2,1/2})$	0.65	4.51
$He^*(2^1S_1)$–$Ar^+(^2P_{3/2,1/2})$	0.95	5.13

metastable atom and the interacting ion, both in size (Table 1) and hardness (roughly proportional to the inverse of the polarizability). This contribution, of electrostatic nature, is due to the penetration of the small and hard ion into the large and soft external electronic shell of the metastable atom. A similar effect is well known in the interaction of both excited alkalis and metastable atoms with rare gases [7,8,17,18]. Another example is given by the H_2^+ ion. For this system, the interaction component obtained as the average of the ab initio potential energy curves for the $^2\Sigma_g$ and $^2\Sigma_u$ states [19], which represents the interaction when the "electron resonance" is removed [20], appears indeed to be significantly less attractive than the pure induction, even at distances comparable or larger than 3 Å. Again this is attributed to the penetration of the proton into the 1s orbital of H. Therefore, we chose the following representation of the diabatic potential: a Lennard–Jones [4,8] function, with the potential parameters of Table 2, with the attractive term (essentially an induction contribution) damped when the interatomic distance decreases and the coulombic repulsion grows up. The functional model assumed for the interaction is

$$x = \frac{R}{R_m};$$

$$V(R) = \varepsilon x^{-8} - 2\varepsilon x^{-4} g(x) + \frac{C}{R_m x}[1 - g(x)] \quad (2)$$

with

$$g(x) = \frac{1}{1 + \exp[(x_0 - x)/d]}$$

where $C = 14.4$, the distance is in Å, and the energy in eV. The parameter d is the ratio between the ion diameter and R_m, while x_0 is the sum of the radii of the two partners divided by R_m (Fig. 2 and Table 1). The diabatic potential energy curves for the following entrance and exit channels

$$Ar^*(^3P_2) + He^+(^2S_{1/2}) \rightarrow Ar^+(^2P_{3/2}) + He^*(2^3S_1) \quad (3a)$$

$$Ar^*(^3P_2) + He^+(^2S_{1/2}) \rightarrow Ar^+(^2P_{3/2}) + He^*(2^1S_0) \quad (3b)$$

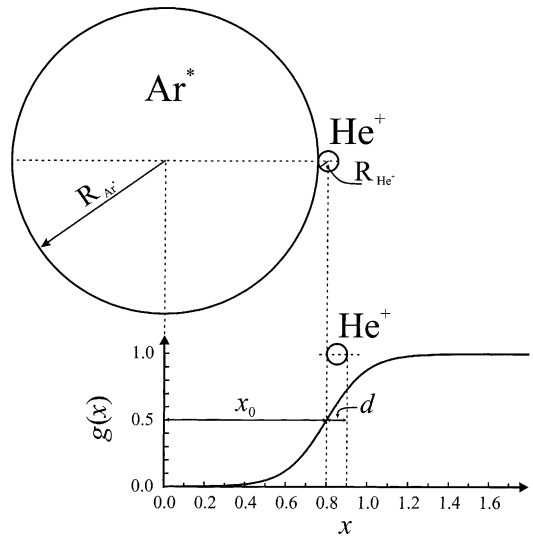

Fig. 2. The damping function $g(x)$ (Eqs. (3a) and (3b)). The radii of the metastable argon atom and of the helium ion are in a relative scale.

and

$$Ar^*(^3P_0) + He^+(^2S_{1/2}) \rightarrow Ar^+(^2P_{1/2}) + He^*(2^3S_1) \quad (4a)$$

$$Ar^*(^3P_0) + He^+(^2S_{1/2}) \rightarrow Ar^+(^2P_{1/2}) + He^*(2^1S_0) \quad (4b)$$

are reported in Fig. 3a and b, respectively. Two entrance and four exit channels are possible, because of the two spin orbit states of the argon ion and the two possible states of He*. However, when the external electron of $Ar^*(^3P_2)$ is removed, only the formation of $Ar^+(^2P_{3/2})$ is possible, while the electron removal from $Ar^*(^3P_0)$ leads exclusively to $Ar^+(^2P_{1/2})$. Thus, for each entrance channel only two exit channels are open, as shown in Fig. 3.

2.2. Coupling terms

Looking at the curves in Fig. 3, one realizes that the crossing distances, where transitions mainly occur, are all confined in the range $4.5\,Å < R < 7.5\,Å$. This allows us to assume that the coupling is mainly due to the electron exchange between the outer orbitals

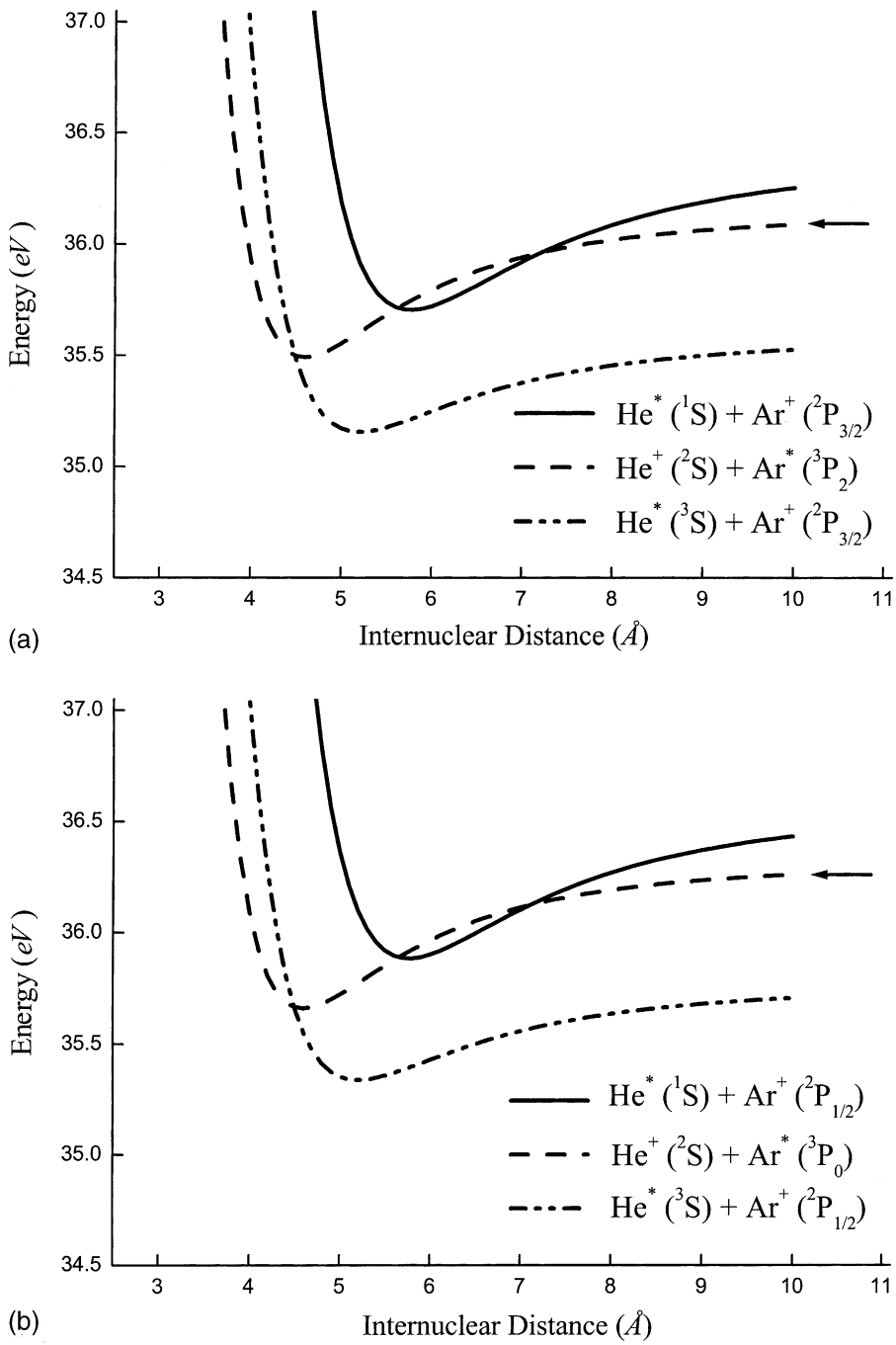

Fig. 3. Diabatic potential energy curves involved in the He^+–Ar^* collisions (a) when the metastable argon atom in the entrance channel is in the $^3P_2$ state and (b) when is in the $^3P_0$ state.

of reagent and product atoms, both in a metastable state. Spin–spin and electronic anisotropy effects are expected to be relevant at short distance and therefore, are not considered in this study. As usual, the dependence on the distance of the coupling term is described by an exponential decreasing function

$$\beta(R) = AR\exp(-\gamma R) \quad (5)$$

where A and γ (Table 3) have been obtained according to recently developed correlation formulas [21,22], which represent an extension and updating of those by Olson et al. [23] and Grice and Hershbach [24] (see also [25]). As far as the reliability of such estimates, it should be noted that the correlation formulas are accurate for systems for which the size of each interacting partner does not change too much as a consequence of the electron exchange. This is not the case for the present system, since the ratio between the radius of He^* and that of He^+ (about $(\alpha_{He^*}/\alpha_{He^+})^{1/3}$) is ∼12 for the metastable helium in the ^3S state, and

Table 3
Parameters for the coupling function $\beta(R)$

	A (eV)	γ (Å^{-1})
$He^+(^2S_{1/2}) + Ar^*(^3P_{2,0})$ → $He^*(2^3S_1)$–$Ar^+(^2P_{3/2,1/2})$	46	1.09
$He^+(^2S_{1/2}) + Ar^*(^3P_{2,0})$ → $He^*(2^1S_1)$–$Ar^+(^2P_{3/2,1/2})$	39	1.04

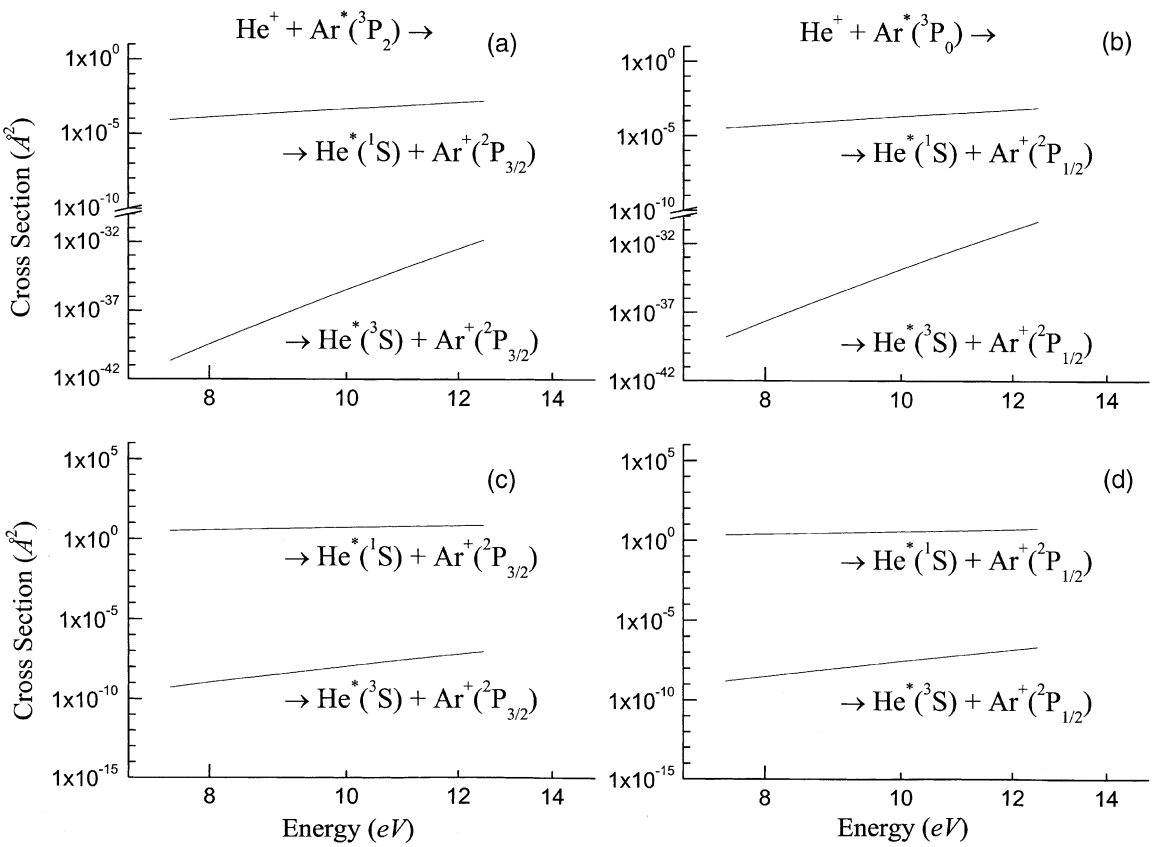

Fig. 4. Calculated cross-sections for the charge exchange reaction between helium ions and metastable argon atoms (a) and (c) when the metastable argon atom is in the $^3P_2$ state, and (b) and (d) when it is in the $^3P_0$ state. Cross-sections shown in panels (a) and (b) are calculated by using coupling terms obtained by correlation formulas, while for cross-sections shown in panels (c) and (d) the same coupling terms have been reduced by a factor 2.

$\sim$16 for the ^{1}S state. Since $\beta(R)$ depends on the value of the overlap integral between orbitals that exchange the electron [21–25], the estimated value, as described before, has to be taken as an upper limit because of the very diffused atomic orbitals involved in the present system. Therefore, some uncertainties characterize the evaluated $\beta(R)$ functions, especially in the value of the A parameter. This is a critical aspect, which should be assessed with particular attention, since the probability of diabatic passage through the crossing R_C exponentially depends on $\beta^2(R_C)$ [26–28] (see following sections).

2.3. Cross-section calculations

For each set of curves (Fig. 3), the positions of the crossings are well separated and therefore, non-adiabatic transitions at each crossing are treated independently. The total probability $P(b)$, for the formation of products in each exit channel at the impact parameter b, is given by an appropriate combination of probabilities of diabatic passage at each crossing, as evaluated by the familiar Landau–Zener–Stückelberg formula [26–28]. In this model, the key quantities are position, energy, difference of slopes at each crossing between potential curves in the diabatic representation, and non-adiabatic β couplings. The cross-section σ, as a function of collision energy E, is obtained by the standard formula

$$\sigma(E) = 2\pi \int_0^\infty bP(b)\,\mathrm{d}b$$

Calculated cross-sections are plotted in Fig. 4a for $He^+ + Ar^*(^3P_2)$ and Fig. 4b for $He^+ + Ar^*(^3P_0)$. As discussed before, for each entrance channel, there are two exit channels, one producing metastable helium in the singlet state and the other one in the triplet state. The exit channel with the helium atom in the singlet state results to be much more efficient than that producing He in the triplet state. This is due to the fact that for the former channel the relevant crossing is located at larger distance, where the coupling is much weaker and non-adiabatic passage is more probable.

Calculated values appear to be quite small and, if correct, this result would be incompatible with the experimental observation of reaction (1). We have, therefore, repeated calculations with the strength of the β coupling reduced by a factor 2 (Fig. 4c and d). Such a reduction results in an increase of the cross-section values.

3. Discussion and conclusions

For many applications and comparisons, it is convenient to give the interaction potential in the adiabatic representation, where diabatic interactions and non-adiabatic couplings are properly combined. In this representation, the bond energy ε' and the equilibrium distance R'_m for the low lying and most stable states of the collision complex, asymptotically correlating with $He^+(^2S) + Ar^*(^3P)$ and with $He^*(^3S) + Ar^+(^2P)$, are estimated to be $\varepsilon' = 0.9$ eV, $R'_m = 4.8$ Å and $\varepsilon' = 0.8$ eV, $R'_m = 4.5$ Å, respectively. It appears interesting to compare such bond features with the dissociation energies D_0 and the equilibrium distances R'_m, listed in Table 4, available for some similar systems, namely symmetric alkali–alkali molecules and ions [29,30]. The similar bond characteristics of the present system and those of ionic alkali diatoms is not surprising, since analogies between metastable rare

Table 4
Dissociation energies, D_0, and equilibrium distances, R'_m, for ionic and neutral alkali diatoms [29,30]

	D_0 (eV)	R'_m (Å)
Li_2	1.05	2.67
Li_2^+	1.44	3.10
Na_2	0.72	3.08
Na_2^+	0.96	3.54
K_2	0.51	3.91
K_2^+	0.85	4.11
Rb_2	0.49	4.17
Rb_2^+	0.72	3.94
Cs_2	0.39	4.47
Cs_2^+	0.61	4.44

For a comparison with the ε' values of the collision complex (see text) the zero point energy should be added to these D_0 values. Such a correction is of the order of $\sim$2% for Li_2 and Li_2^+, and becomes smaller for heavier systems.

gases and alkali atoms and between the corresponding ions are in fact well known [7–9]. It is interesting to note an intriguing feature of the alkali diatomic molecules: when passing from the neutral to the ionic state, the equilibrium distance remains comparable or becomes even larger, while the bond strength always increases although an electron is removed from the bonding molecular orbital. The interaction model used in the present investigation provides a simple and natural explanation of such a feature. In fact, the induction attraction term does not exist in the neutral dimer, and therefore, size repulsion and electron exchange are dominant. In contrast, size repulsion and electron exchange effects are significantly lower in the diatomic ion, while coulombic repulsion due to penetration effect is operative only at short range. On the other hand, for the ionic system the induction term is dominant at large and intermediate distances, due to the strong interaction between the cation and the induced multipole on the alkali atom. These combined effects make the bond in the ionic diatom stronger than in the neutral one, a counter-intuitive result when one considers the chemical bond as resulting from the increased electron density between the nuclei.

On the basis of the previous considerations, we can understand some features of the collision complex in reaction (1). At large distance, the interacting complex can be seen as a simple ion–neutral atom system. When the two partners approach each other, the probability of electron exchange increases, leading to a partial electron mobility within the complex. This effect controls the reaction probability: at large distance the coupling is weak, the electron mobility is low, and the reaction is highly probable. At even shorter distances, the coulombic repulsion arises while the electron increases further its mobility, and the complex can be seen as a diatomic dication surrounded by one electron in a Rydberg molecular state.

Acknowledgements

The present work has been part of a European project within the MCInet Research Training Network (contract No. HPRN-CT-2000-00027). Financial contributions from ASI (Agenzia Spaziale Italiana) and from ENEA (Ente per le Nuove Tecnologie, l'Energia e l'Ambiente) are gratefully acknowledged.

References

[1] M.I. Boulos, P. Fauchais, E. Pfender, Thermal Plasmas, Plenum Press, New York, 1994.
[2] J.R. Roth, Industrial Plasma Engineering, Institute of Physics Publishing, London, 1995.
[3] P. Tosi, D. Bassi, B. Brunetti, F. Vecchiocattivi, Int. J. Mass Spectrom. Ion Process. 149/150 (1995) 345.
[4] C. Riccardi, R. Barni, M. Fontanesi, P. Tosi, Chem. Phys. Lett. 329 (2000) 66.
[5] B. Christensen, T.L. Patterson, T.A. Tinsley, J. Geophys. Res. 76 (1971) 1764.
[6] T.B. Cook, W.P. West, F.B. Dunning, R.D. Rundel, R.F. Stebbings, J. Geophys. Res. 79 (1974) 678.
[7] B. Brunetti, F. Vecchiocattivi, in: C.Y. Ng, T. Baer, I. Powis (Eds.), Cluster Ions, Wiley, New York, 1993, p. 359.
[8] P.E. Siska, Rev. Mod. Phys. 65 (1993) 337.
[9] K. Ohno, in: Y. Itakawa, K. Okuno, H. Tanaka, A. Yagishita, M. Matsuzawa (Eds.), The Physics of Electronic and Atomic Collisions, American Institute of Physics, Conference Proceedings 500, New York, 2000, p. 677.
[10] P. Tosi, Chem. Rev. 92 (1992) 1667.
[11] V. Aquilanti, D. Cappelletti, F. Pirani, Chem. Phys. 209 (1996) 299.
[12] H. Haberland, Y.T. Lee, P.E. Siska, Adv. Chem. Phys. 45 (1981) 488.
[13] G. Liuti, F. Pirani, Chem. Phys. Lett. 122 (1985) 245.
[14] T.K. Ganthy, S.K. Ghosh, J. Phys. Chem. 100 (1996) 17429.
[15] R. Cambi, D. Cappelletti, G. Liuti, F. Pirani, J. Chem. Phys. 95 (1991) 1852.
[16] D. Cappelletti, G. Liuti, F. Pirani, Chem. Phys. Lett. 183 (1991) 297.
[17] W.E. Baylis, J. Chem. Phys. 51 (1969) 2665.
[18] J. Pascale, J. Vandenplanque, J. Chem. Phys. 60 (1974) 2278.
[19] W. Kolos, L. Wolniewicz, J. Chem. Phys. 43 (1965) 2429.
[20] L. Pauling, J. Chem. Phys. 1 (1933) 56.
[21] V. Aquilanti, D. Cappelletti, F. Pirani, J. Chem. Phys. 106 (1997) 5043.
[22] F. Pirani, A. Giulivi, D. Cappelletti, V. Aquilanti, Mol. Phys. 98 (2000) 1749.
[23] R.E. Olson, F.T. Smith, E. Bauer, Appl. Opt. 10 (1971) 1848.
[24] R. Grice, D.R. Hershbach, Mol. Phys. 27 (1974) 159.
[25] E.E. Nikitin, A.I. Reznikov, S.Y. Umanskii, Mol. Phys. 65 (1988) 1301, and reference therein.
[26] L.D. Landau, Phys. Zts. Sowjet. 2 (1932) 46.
[27] C. Zener, Proc. R. Soc. A 137 (1932) 696.
[28] E.C.G. Stückelberg, Helv. Phys. Acta 5 (1932) 369.
[29] K.P. Huber, G. Herzberg, Molecular Spectra and Molecular Structure IV Constants of Diatomic Molecules, van Nostrand, Priceton, NJ, 1979.
[30] A.A. Radzig, B.M. Smirnov, Reference Data on Atoms, Molecules, and Ions, Verlag, Berlin, 1985.